

# Chapter 21

## Multiphysics Modelling of Innovative Food Processing Technologies

Pablo Juliano and Kai Knoerzer

### 21.1 Introduction

The food industry is an increasingly competitive and dynamic arena with consumers being more aware of what they eat and, more importantly, what they want to eat. Important food quality attributes such as taste, texture, appearance, and nutritional content are strongly dependent on the way foods are processed (Knoerzer et al. 2011b).

In recent years, a number of innovative food processing technologies, also referred to as “emerging” or “novel” technologies have been proposed, investigated, developed, and implemented with the aim to improve or replace conventional processing technologies. These technologies take advantage of other physics phenomena such as static high hydrostatic pressure or dynamic pressure waves, or electric and electromagnetic fields, and provide the opportunity for the development of new foods, but also for improving the quality of established food products through gentle processing. The physical phenomena utilized by these technologies can potentially reduce energy and water consumption and, therefore, can play an important role towards environmental sustainability of food processing and global food security by expanding the shelf stable product spectrum (Knoerzer et al. 2011b).

Apart from the underlying thermo- and fluid-dynamic principles of conventional processing, these innovative technologies incorporate additional Multiphysics dimensions, for example, pressure waves, electric and electromagnetic fields, among others. To date, they still lack an adequate, complete understanding of the basic principles of intervening in temperature and flow evolution in product and equipment during processing (Barbosa-Canovas et al. 2011). The development and optimization of suitable

---

P. Juliano • K. Knoerzer (✉)  
CSIRO Animal, Food and Health Sciences, Melbourne, VIC, Australia  
e-mail: [kai.knoerzer@csiro.au](mailto:kai.knoerzer@csiro.au)

equipment and process conditions that provide the adequate uniformity still remains a challenge. Computational Fluid Dynamics (CFD) is an established tool for characterizing, improving and optimizing traditional food processing technologies; the partial differential equations solved are those describing the conservation of mass, momentum, and energy (i.e., Continuity, Navier–Stokes, and Fourier equations). Innovative technologies, however, provide additional complexity and challenges for modellers because of the concurrent interacting Multiphysics phenomena; further partial differential equations need to be solved simultaneously, such as the Maxwell's and the constitutive equations for problems involving electromagnetics (e.g., microwave and radiofrequency processing), charge conservation (e.g., pulsed electric field processing), and wave equations (e.g., Helmholtz wave equations) for ultrasonic and megasonic processing (Knoerzer et al. 2011b). These equation systems can increase in complexity when not only the process variables are to be predicted, but also process outcomes such as microbial/enzyme inactivation or food matrix modification. In such cases the numerical problem is coupled to equations describing the dynamics of occurrence of such phenomena, e.g., inactivation, the development of (acoustic) forces leading to transport of concentrated species, among others.

## 21.2 Simulating Innovative Food Processing Technologies

A common problem of innovative food processing technologies is the nonuniformity of the treatment, which can be caused by gradients of process variables such as temperature, electric field strength, or sound pressure fields in the processing chambers. A nonuniform distribution of a certain process variable leads to nonuniformities in the resulting outcomes of the process (e.g., microbial inactivation).

While trial-and-error optimization is always an option to improve equipment and process design, it is the least preferred way, as it is very cost-, labor-, and time-intensive and a good performance may be missed, as not all possibilities can be tested following this approach. On the other hand, numerical modelling using CFD can be used exactly for this purpose at reduced cost and time of equipment use. This way, advantages and disadvantages of the respective technology can be identified and either utilized or minimized.

Numerical modelling studies have been reported across the range of innovative food processing technologies, such as microwave and radiofrequency, ultraviolet light, high pressure (thermal), pulsed electric field, and ultrasonics/megasonics processing.

The common objective of microwave and radiofrequency processing is the temperature increase in the treated product, e.g., for the purpose of thermal pasteurization, sterilization, preheating, cooking, thawing, and drying. Numerical studies on microwave processing have been reported, for example by (Birla et al. 2008; Tiwari et al. 2011; Geedipalli et al. 2007; Knoerzer et al. 2008).

Unlike microwave and radiofrequency processing, ultraviolet light for treating liquid products or product surfaces is a nonthermal process utilized mainly for the

purpose of inactivation of microorganisms. Modelling studies have been reported, for example by (Huachen and Orava 2007; Unluturk et al. 2004).

The following sections highlight in more detail the latest advances in modelling high pressure thermal, pulsed electric field and ultrasonics/megasonics processing. These technologies have been investigated in more detail by our group and therefore become the focus of the following sections.

### 21.2.1 High Pressure Thermal Processing

High pressure thermal processing is a technology that is effective in inactivating not only vegetative organisms but also microbial spores, due to the elevated temperatures involved. Because the process time can be reduced compared to thermal-only processing through rapid compression heating and decompression cooling, quality attributes, such as color, nutrients, flavor, and texture can be better retained (Olivier et al. 2011).

A number of studies have been reported on the utilization of Multiphysics modelling for equipment and process characterization in terms of process temperature and flow field distributions (Knoerzer et al. 2007; Knoerzer and Chapman 2011), prediction of microbial (spore) inactivation (Juliano et al. 2009), and equipment optimization (Knoerzer et al. 2010) (Fig. 21.1).

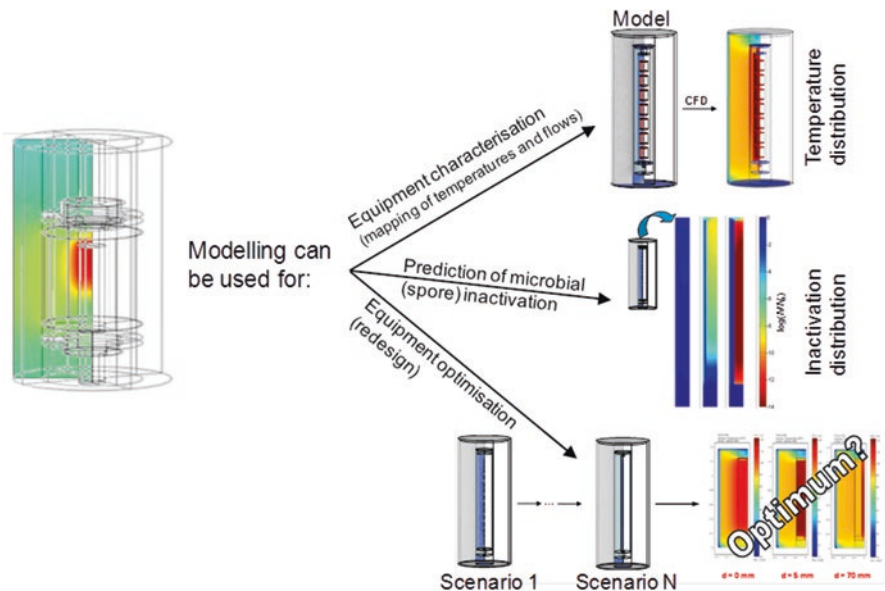


Fig. 21.1 Applications of numerical models describing high pressure thermal processing

Knoerzer et al. (2007) reported on the use of a numerical model to describe temperature and flow distribution in a 35 L pilot scale high pressure sterilization system (Avure Technologies Inc., Seattle, WA, USA) and evaluated the differences of the process variables for a number of different product carriers made of metal and insulating plastic material. Figure 21.2 shows the temperature distributions in three investigated scenarios at the end of pressurization, namely a cylindrical steel high pressure vessel without carrier, one with a metal carrier and one scenario where a carrier made from insulating PTFE was placed into the vessel.

As shown in the figure, the temperature distribution achieved in scenario (a) shows nonuniformities and relatively low temperatures compared to the scenarios where carriers are included, which avoid pronounced cooling down caused by the incoming pressurization fluid. Temperatures in scenario (b) are more uniform but still lower than in scenario (c). Furthermore, during pressure hold time, scenarios (a) and (b) exhibit pronounced heat losses, whereas the PTFE carrier in scenario (c) was able to retain the heat inside the carrier.

As expected, only the insulated carrier provided process conditions feasible for sufficient and uniform product sterilization through microbial spore inactivation (Fig. 21.3).

Juliano et al. (2009) applied more detailed models (Fig. 21.4a) describing the process variables (i.e., pressure, temperature, and flow) and evaluated the differences in the extent and distribution of predicted inactivation of *Clostridium botuli-*

**Fig. 21.2** Temperature distribution in an axis-symmetric section of the cylindrical high pressure vessel; (a) no carrier in the vessel, (b) inclusion of cylindrical metal carrier, (c) inclusion of cylindrical PTFE carrier; at the end of pressurization

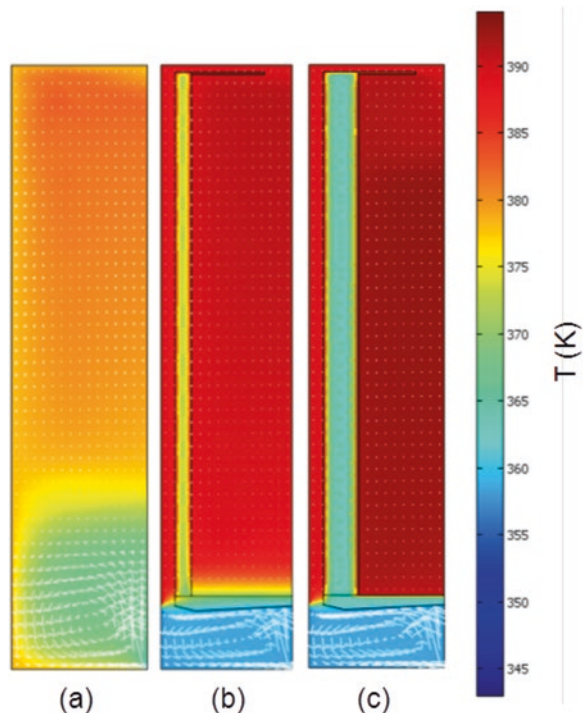


**Fig. 21.3** Distribution of *Clostridium botulinum* spore inactivation as predicted by the log-linear model in (a) the vessel without product carrier, (b) the vessel including a steel carrier, and (c) the vessel including a PTFE carrier

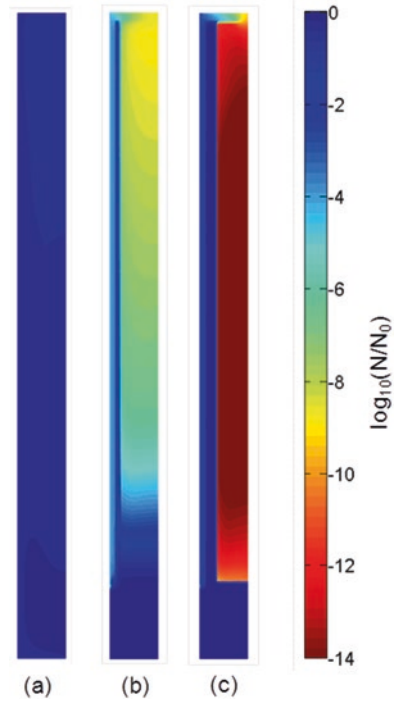
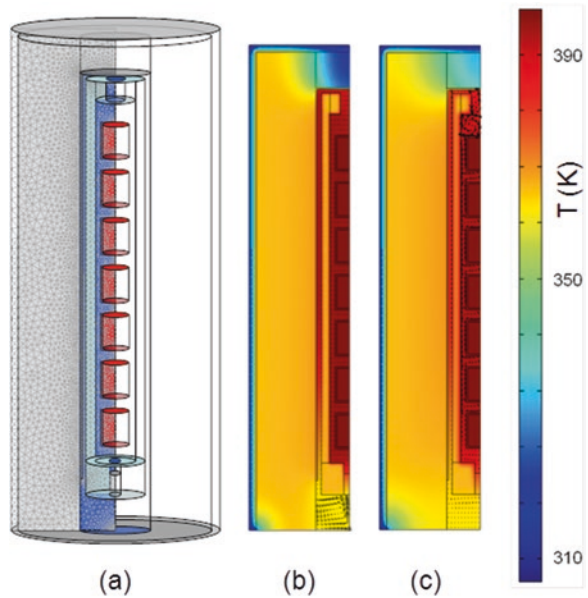


**Fig. 21.4** Model geometry (a) and predicted temperature distributions at the end of pressurization (b) and pressure hold time (c)

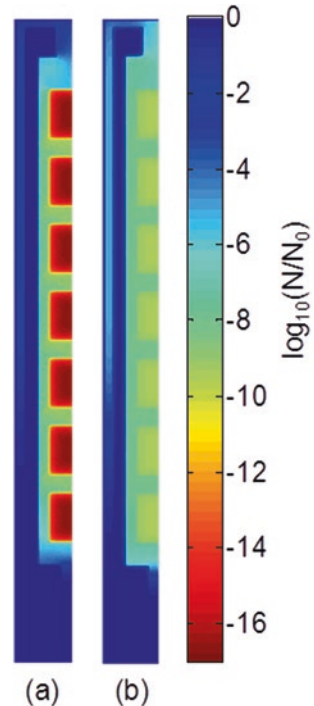


num spores in food packages. In a first step, the CFD models were able to show heat retention inside the food packs and temperature magnitudes of  $\sim 121$  °C during pressure hold time (Fig. 21.4b, c).

The predicted transient temperature distributions were then coupled to selected predictive microbial inactivation models, namely, the commonly known log-linear model, an  $n$ -th order model and a Weibull distribution model. The different inactivation models predicted very different levels of spore inactivation for the same pressure and temperature conditions. For example, the log-linear model predicted inactivation of *C. botulinum* spores in the order of 16  $\log_{10}$  after 3 min processing at 600 MPa and 121 °C (Fig. 21.5a), whereas the Weibull model indicated spore inactivation of only 9  $\log_{10}$  for the same process (Fig. 21.5b). The inactivation model used ultimately will affect the selection of optimum process conditions for a HPT process. The determination of the most appropriate microbial inactivation model for HPT products manufacture needs further study.

Knoerzer et al. (2010) then used a modified version of the model to optimize the wall thickness of the insulating carrier while increasing product load capacity. The carrier supplied by the manufacturer was designed with a wall thickness such that sufficient heat retention was ensured during processing. The authors derived a dimensionless parameter, referred to as the Integrated Temperature Distributor (ITD) value (Eq. 21.1) to evaluate temperature uniformity, and the temperature magnitude expressed relative to a target temperature and heat retention during processing.

**Fig. 21.5** Indication of inactivation of *C. botulinum* spores as predicted by the log-linear model (a) and the Weibull distribution model (b)



$$ITD = \frac{\int_{r_{min}}^{r_{max}} \int_{z_{min}}^{z_{max}} 10^{\frac{\int_0^t r(t) dt}{t_{process} - T_{target} z_r}} dr dz}{(r_{max} - r_{min}) \cdot (z_{max} - z_{min})} \tag{21.1}$$

where  $r_{min}$ ,  $r_{max}$ ,  $z_{min}$ ,  $z_{max}$  cover the region of interest (the carrier volume),  $t_{process}$  is the process time of interest (in this case, the pressure holding time where most of the heat loss is expected) and  $T_{target}$  is the targeted holding temperature of the process under pressure.

An iterative strategy was applied, which consisted of a model that automatically changed the carrier wall thickness in a range of 0–70 mm, and evaluated temperature performances and load capacities for the respective scenarios. Figure 21.6 shows the modified model geometry with variable carrier wall thickness and the predicted temperature distributions at the end of pressure hold time for a wall thickness of 0, 5 and 70 mm.

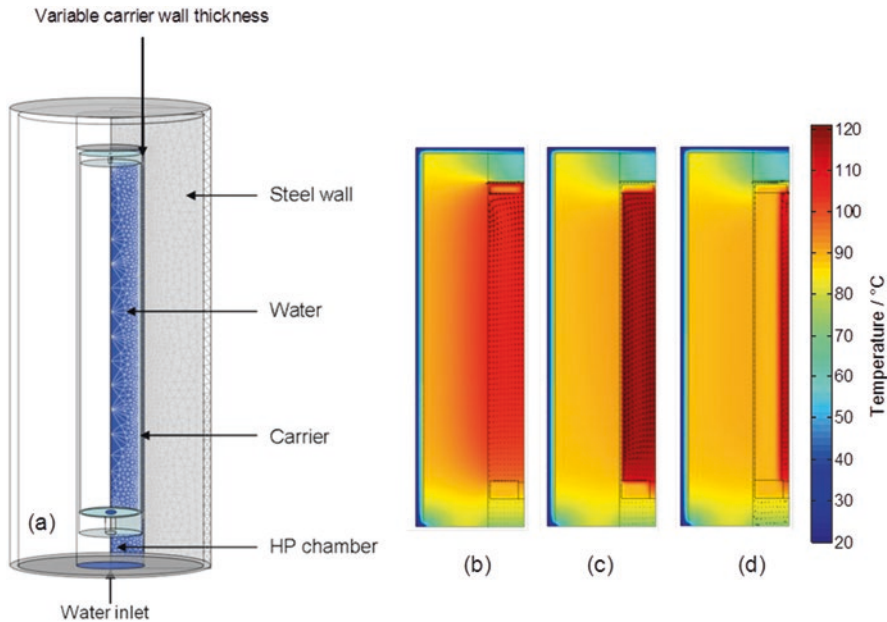


**Fig. 21.6** Depiction of modified model geometry (a) and the predicted temperature distributions at a wall thickness of 0 mm (b), 5 mm (c), and 70 mm (d)

The study showed that the wall thickness can be reduced from 28 mm to approximately 4 mm without compromising temperature performance, leading to an increase of carrier load capacity by more than 100 % (Fig. 21.7).

### 21.2.2 Pulsed Electric Field Processing

Pulsed Electric Field (PEF) processing is a technology that can be applied for cold or low temperature pasteurization of liquid products. It is able to inactivate vegetative microorganisms through the application of electric fields in the order of several ten thousand volts per centimeter for a very short time, leading to cell poration and cell death (Heinz et al. 2003). Overall treatment times are in the order of microseconds. Other potential applications of this technology are for enhanced extraction processes or softening of fruit and vegetable tissue, for example for improving cutting performance and reducing cutting losses. Also, this technology can improve the quality attributes of foods compared to conventional thermal processing, such as flavor, color, and nutrients, among others. Being a continuous process, high throughputs are possible.

Published studies on numerical modelling of pulsed electric field processing include the utilization of such models for equipment characterization with respect to electric field, temperature and flow distribution (Buckow et al. 2010, 2011), the

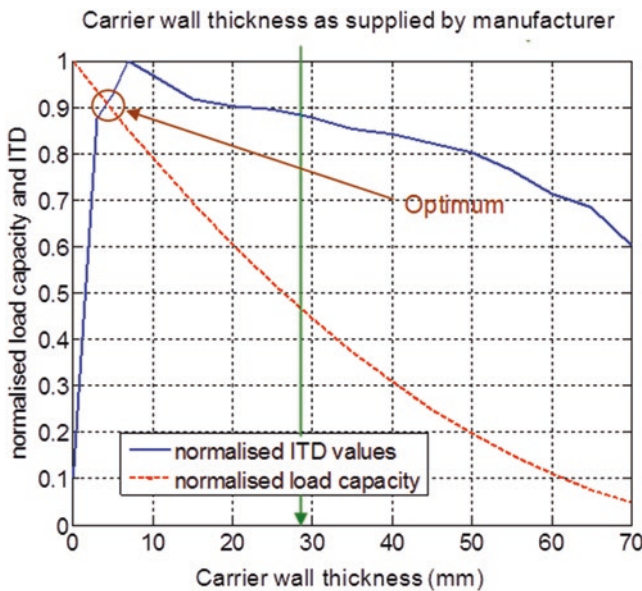


Fig. 21.7 Determination of optimum carrier wall thickness by evaluating temperature performance (ITD) and load capacity of the carriers with varying wall thickness



prediction of microbial or enzyme inactivation (Buckow et al. 2012; Knoerzer et al. 2011a) and equipment optimization to ensure uniform and effective processing (Knoerzer et al. 2012) (Fig. 21.8).

Buckow et al. (2010) reported on the development of a 3D model for a pilot scale pulsed electric field system (Diversified Technologies Inc., Bedford, MA, USA) to predict electric field strength, flow, and temperature distributions (Fig. 21.9) and an extensive validation of the model predictions through temperature measurements within the constrained space of the treatment chamber’s active zone and the second ground electrode (Fig. 21.10). The authors investigated the treatment of salt solutions with different conductivities and whole milk, processed at two flow rates, and five different inlet temperatures. Pulses were applied at two different voltage settings, four pulse repetition rates, and three pulse widths. They were able to utilize this model to characterize and evaluate the performance of the system as supplied by the manufacturer with respect to electric field strength, temperature and flow distribution.

Buckow et al. (2011) applied this model further to derive simplified equations to estimate accurate electric field strengths and specific energy inputs from treatment variables such as voltage, pulse frequency and duration, among others. Also evaluated were the effects of changing treatment chamber geometry and configuration on these process variables. A common approach for estimating electric field strength is

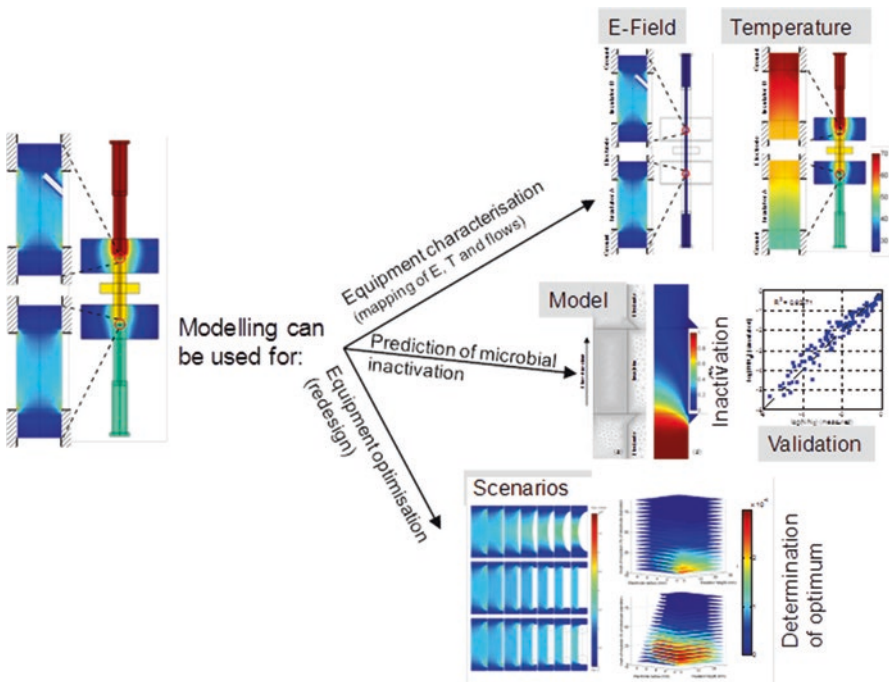
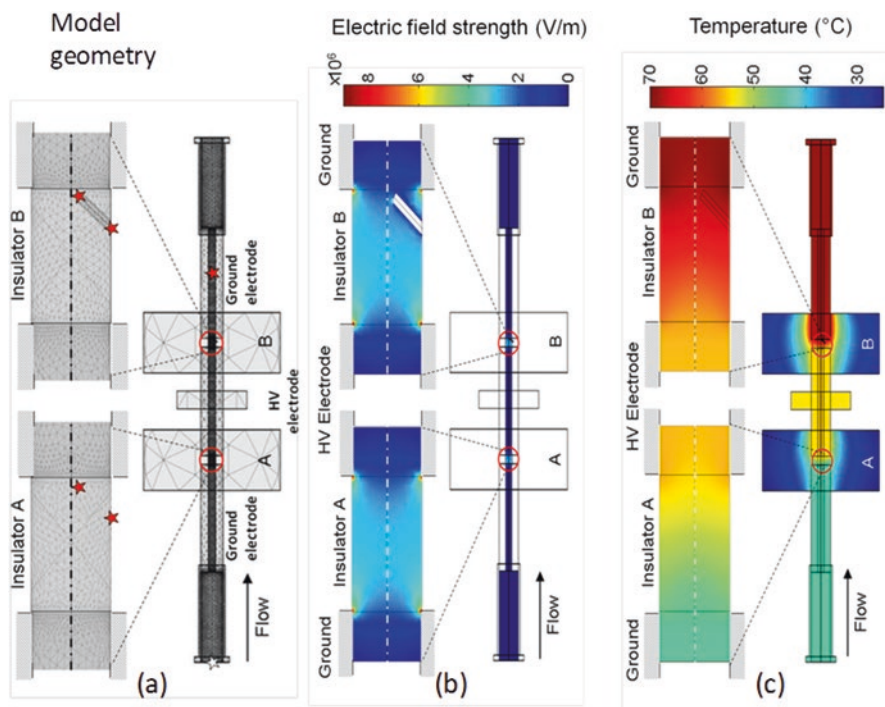


Fig. 21.8 Applications of numerical models describing pulsed electric processing



**Fig. 21.9** Representation of the pilot scale treatment chamber including magnification of the treatment zones (model geometry **a**), electric field strength distribution in a salt solution at 4 mS/cm, flow rate of 4 L/min, inlet temperature of 45  $^{\circ}\text{C}$ , voltage of  $\sim 22$  kV, pulse width of 5  $\mu\text{s}$ , and frequency of 600 Hz (**b**), and temperature distribution at these conditions (**c**)

relating the applied voltage to the electrode gap. While this will give accurate predictions for parallel plate systems, it was found that for configurations used in continuously operating systems, such as co-field or co-linear design, this approach always over-predicts the actual electric fields. This is similar for specific energy input, commonly estimated by multiplying voltage, current, pulse width, pulse repetition rate and mass flow. Figure 21.11 shows (a) the correlation of relative electric field strength (i.e., actual electric field strength/estimated electric field strength for parallel plate configuration) and (b) the correlation of the relative specific energy input (i.e., the actual specific energy input/estimated specific energy input for parallel plate configuration) with the ratio of electrode radius and electrode gap for different chamber configurations. These configurations were: “no inset” (where the insulator bore diameter is equal to the inner electrode diameter), “rectangular inset” (where the insulator bore diameter is smaller than the inner electrode radius), “chamfer edge inset” (which is identical to the rectangular inset with rounded edges of the insulator bore), and “elliptical inset” (where the insulator bore has an inward concave shape); see also Fig. 21.13.

**Fig. 21.10** Validation of the model for different fluids and ~50 process conditions (over 400 data points)

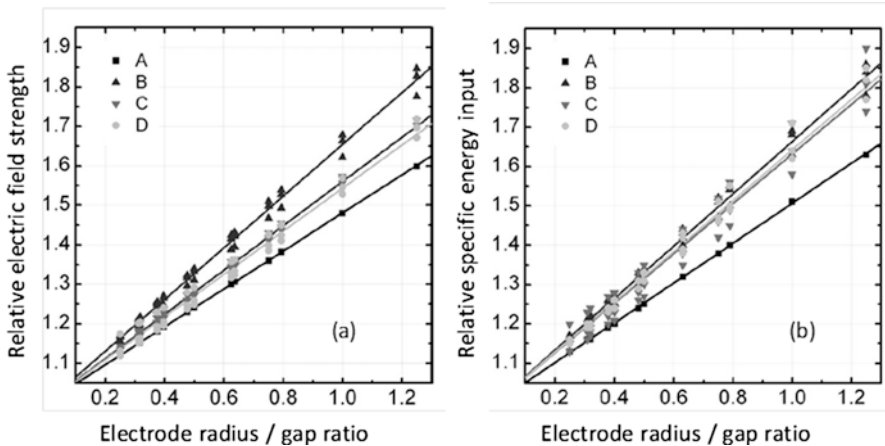
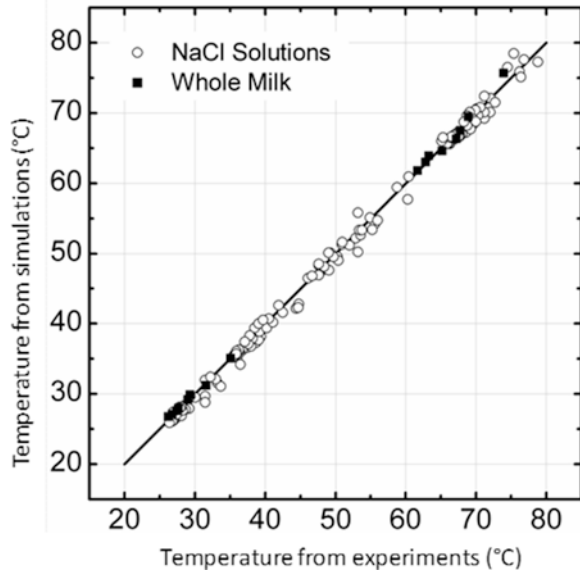


**Fig. 21.11** Correlation of (a) the relative electric field strength and (b) the relative specific energy input with the ratio of electrode radius and gap for “no inset” (A), “rectangular inset” (B), “chamfer edge” (C), and “elliptical inset” (D) chamber configurations

Buckow et al. (2012) then developed and validated a model for a laboratory scale pulsed electric field system (Fig. 21.12a) and evaluated the effect of the electric field on lactoperoxidase (LPO) degradation (an indicator for pasteurization) by coupling the predicted temperature distributions (e.g., Fig. 21.12c) to predictive LPO degradation models accounting for the thermal component only.

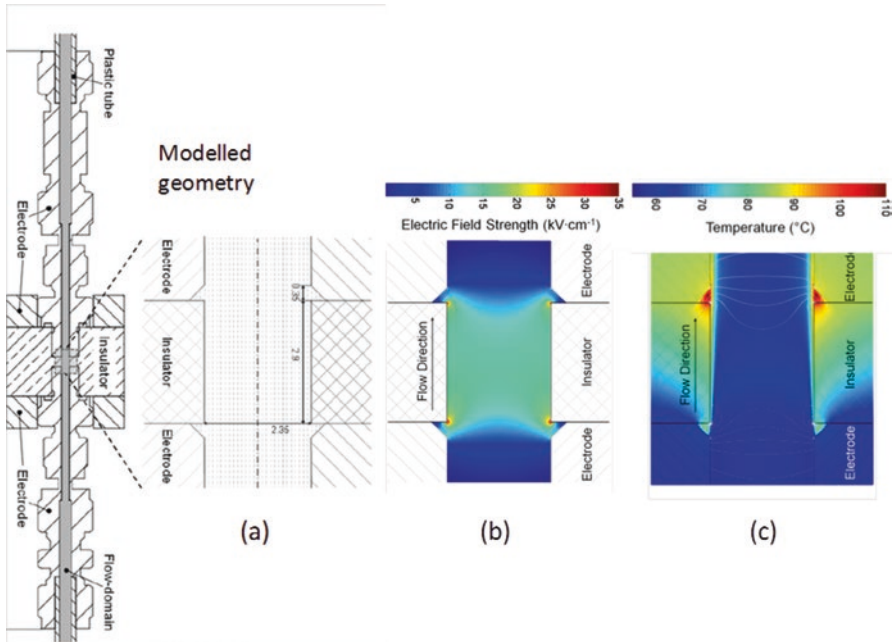


**Fig. 21.12** Representation of the modelled geometry of the lab scale PEF system (a), predicted electric field distribution (b), and predicted temperature distribution (c)

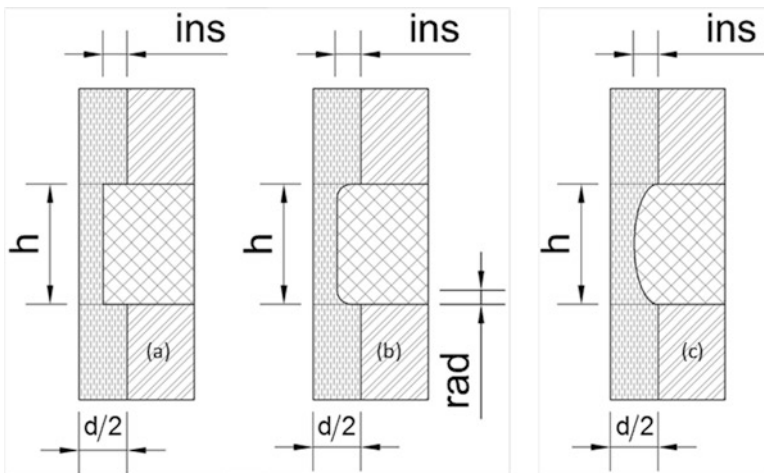


**Fig. 21.13** Investigated chamber configurations, indicating the geometrical parameters varied in the model; (a) rectangular inset, (b) rectangular chamfered edge inset, and (c) elliptical inset scenario

The study indicated that the major effect for LPO inactivation comes from the elevated process temperatures as the predictions (thermal only degradation) were close to the measured degradation (combined thermal and PEF) for a number of process conditions; however, they found that some additional inactivation was also caused by the electric field of up to 12 % potentially caused by the high intensity electric pulses and induced electrochemical reactions.

Lastly, Knoerzer et al. (2012) developed an iterative algorithm that was capable of automatically changing the treatment chamber configuration and dimensions in the Multiphysics models and to identify, out of more than 100,000 scenarios, the one that showed the highest degree of electric field uniformity, together with sufficient throughput, lowest pressure drop, among other evaluation characteristics. The evaluation of the performance of the models was based on a parameter, referred to as the Dimensionless Performance Parameter (DPP), calculated by an equation derived by the authors (Eq. 21.2), accounting for the treatment volume, pressure drop estimations, electric field magnitude related to that achievable in parallel plate systems, electric field uniformity, and peaks of the electric field strength.

$$\text{DPP} = \left( \frac{V_{\text{zone}}}{V_{\text{max}}} \right)^{a_1} \cdot \left( \frac{(d - \text{ins})^4}{d^4} \right)^{a_2} \cdot \left( \frac{E_{\text{av}}}{V_0} \cdot \frac{V_0}{h_{\text{min}}} \right)^{a_3} \cdot \left( \frac{n_{\text{av} \pm 10\%}}{n_{\text{total}}} \right)^{a_4} \cdot \left( \frac{E_{\text{av}}}{E_{\text{max}}} \right)^{a_5} \quad (21.2)$$

where  $V_{\text{zone}}$  is the volume of the treatment zone (insulator region) of the respective scenario,  $V_{\text{max}}$  the volume of the largest treatment zone considered,  $E_{\text{av}}$  is the average electric field strength of the insulator region,  $V_0$  the applied potential,  $h_{\text{min}}$  the minimum electrode distance (gap) of all scenarios investigated,  $n_{\text{av} \pm 10\%}$  the number of elements in the treatment zone with electric field strengths within 10 % of the average electric field strength,  $n_{\text{total}}$  the total number of elements in the treatment zone and  $E_{\text{max}}$  the maximum electric field strength in the respective scenario;  $a_1$ – $a_5$  are weighing parameters adjustable depending on the importance on the respective performance variable.

Three different chamber configurations (Fig. 21.13) were studied and for each of these, four different geometry parameters were varied, with the internal diameter  $d$  of the electrodes ranging from 2 to 20 mm, the height  $h$  of the electrode gap ranging from 1 to 30 mm, a total inset  $\text{ins}$  (i.e., the internal diameter of the insulator) in a range of 0–90 % of the electrode diameter  $d$ , and for the “rectangular rounded edge inset” models also the chamfer radii  $\text{rad}$  ranging from 0 to 40 % of the diameter reduction  $\text{ins}$  (Fig. 21.13).

The algorithm first generated the models, then solved them, applied the performance evaluation by utilizing the DPP equation and then identified the scenario which yielded the highest DPP value, which was found for configuration (b). The authors then set up a full 3D model of this configuration, built the new chamber and performed validation studies of the model for a salt solution and apple juice and for

various process conditions. They found that the new design could be predicted well with respect to the temperatures generated in the treatment chamber (Fig. 21.14).

### 21.2.3 Ultrasonics and Megasonics Processing

Ultrasound processing spans over a wide range of acoustic frequencies, starting as low as 18 kHz, up to several MHz. Applications are as diverse as the frequency spectrum is wide. At the lower frequency (18–200 kHz) end (also known as ultrasonics) the effects are caused mainly by instable cavitation. Traditional applications such as emulsification, cleaning, extraction (Gogate and Kabadi 2009), and more novel applications used for improved drying (Sabarez et al. 2012) and beverage defoaming (Rodriguez et al. 2010) in airborne ultrasound systems can be listed. When using higher frequencies (>0.2 MHz, also known as megasonics), the effects can be either mechanical through standing pressure waves and microstreaming, and/or sonochemical (radical driven) or biochemical (stress response in living tissue). Novel high frequency applications include the separation of particles in standing wave systems (Juliano et al. 2013), and texture improvement of processed fruits and vegetables, through produce-internal stress responses (Day et al. 2012).

Published studies on numerical modelling of ultrasonics and megasonics processing include the utilization of Multiphysics models for equipment characterization with respect to acoustic pressure, temperature, and flow distribution (Trujillo

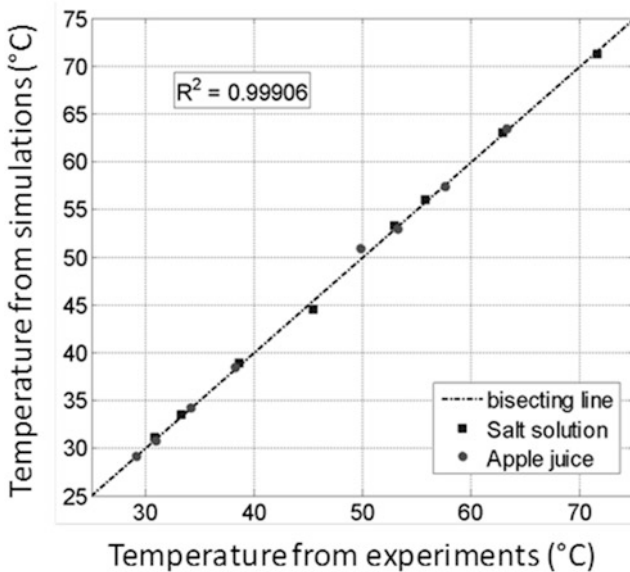


**Fig. 21.14** Parity plot of predicted and experimentally determined temperature values in the new treatment chamber

and Knoerzer 2009, 2011), equipment optimization (Trujillo and Knoerzer 2009) and for predicting particle separation in megasonics standing wave applications (Trujillo et al. 2013) (Fig. 21.15).

Trujillo and Knoerzer (2011) reported on the development of a Multiphysics model capable of simulating the formation of a sound pressure jet produced by a sonotrode placed in water in a low frequency (20 kHz) high power ultrasound application. The acoustic power was dissipated within close proximity to the horn and the acoustic energy was completely converted into kinetic and thermal energy leading to a jet being formed and directed away from the sonotrode while the temperature was increasing in the bulk of the treated fluid. The model was validated by utilizing published data (Kumar et al. 2006) where fluid movement was measured by Laser Doppler Anemometry.

Figure 21.16 shows the computational representation of the system investigated by Kumar et al. (2006) and Trujillo and Knoerzer (2011) in 3D and 2D. Full 3D and axis-symmetric 2D models predicted almost identical values; therefore, and the fact that the computational demand of the 3D model was very high, all further models for comparison with the LDA data were solved in 2D only. Figure 21.17 shows a direct comparison of the velocity profile predicted by the model and the one measured by LDA for a specific power input of 35 kW/m<sup>3</sup>. Both prediction and measurement show the jet being formed underneath the horn tip with much lower velocities throughout the rest of the reactor.

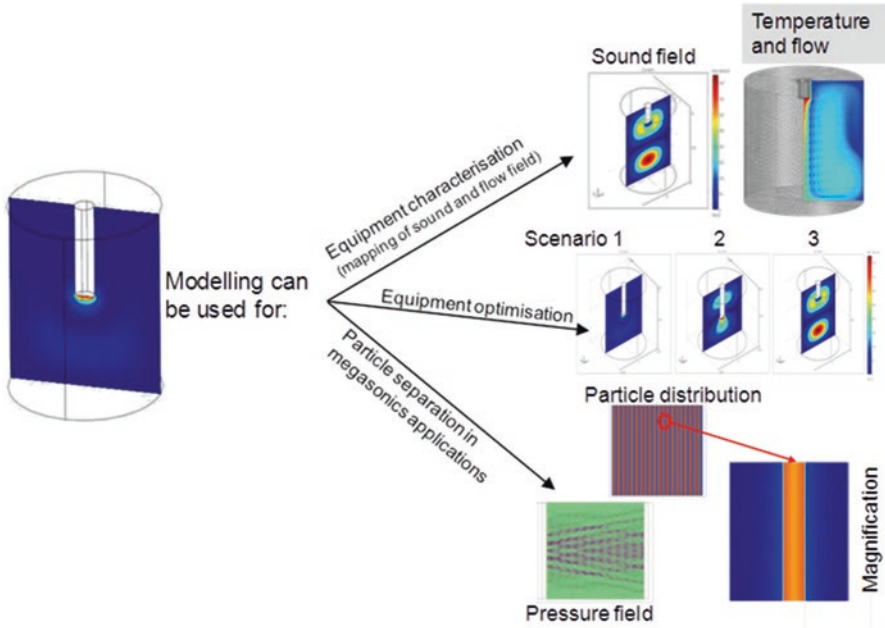


**Fig. 21.15** Applications of numerical models describing low and high frequency ultrasound processing

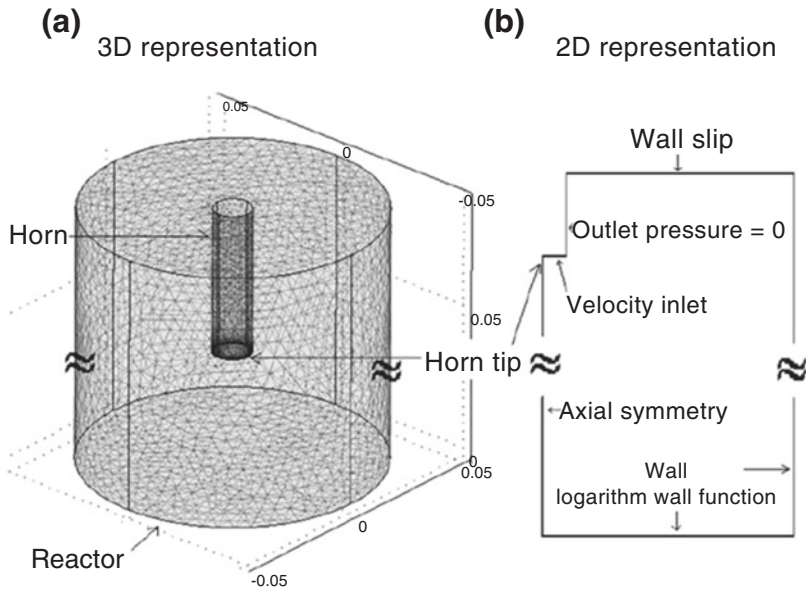


**Fig. 21.16** Depiction of the geometry of the investigated system; (a) 3D representation, (b) 2D axis-symmetric representation, including the boundary conditions of the model

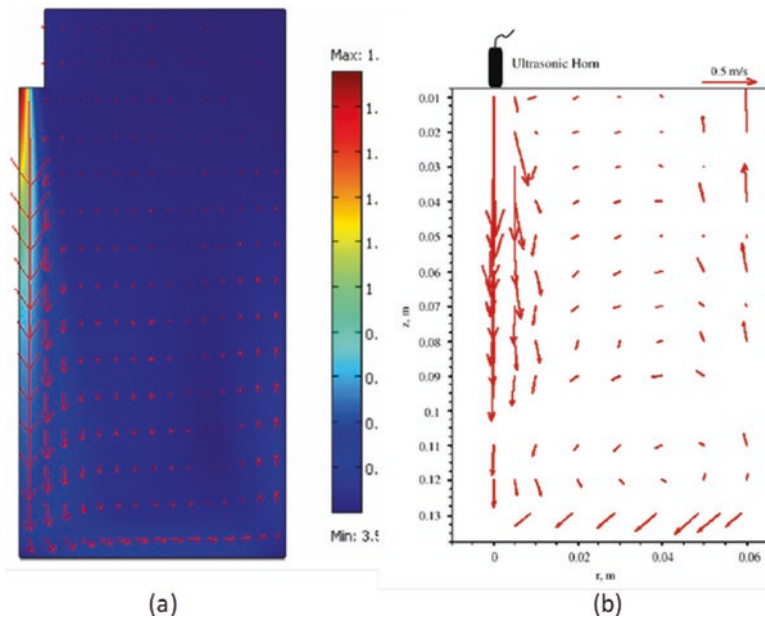


**Fig. 21.17** Visual comparison of the predicted (a) and measured by LDA (b) flow profiles in the investigated system at a specific power input of 35 kW/m<sup>3</sup>. The scale is defined by an *arrow* at the top right hand corner with a unit value of 0.5 m/s



In addition to visual comparisons, the authors also performed a quantitative validation of the model by comparing the predicted values of the axial velocity at a number of heights and radii (Fig. 21.18) and found good agreement.

Apart from low frequency ultrasound applications, Trujillo et al. (2013) have also published research on the development of a Multiphysics model for a high frequency ultrasound application for separation of particles out of a continuous water phase. The simulated separation reactor is shown in Fig. 21.19a. The model included solving for the mechanical displacement of the reactor walls, leading to the formation of an acoustic pressure field (indicated in Fig. 21.19a for a fixed frequency of 1.54 MHz as a thin band in the reactor and a magnified view in Fig. 21.19b,  $p$ ), followed by predicting the acoustic radiation force acting on suspended particles (Fig. 21.19b,  $F_{\text{Rad}}$ ). Finally, this (transient) force was utilized to solve for the movement of the particle phase to the nodes of the ultrasonic standing wave (Fig. 21.19b,  $X_p$ ) and frequency ramping, leading to active separation of the particles away from the transducer plate towards the reflector.

The authors then compared digitized images of the actual process at discrete times of 0, 40, and 120 s (Fig. 21.20a) with the predicted particle band formation and transient band movement. As shown in Fig. 21.20b at a discrete time of 120 s, measurement and predictions agreed well. Figure 21.21 shows a parity plot of the measured and predicted band locations for all three time steps; as can be seen, very good agreement was found.

### 21.3 Summary and Outlook

It is widely established that innovative technologies are the means to meet a need and capture an opportunity, particularly around the manufacture of attractive, new, high quality products with fresh-like quality attributes, ensured safety, and long shelf-life, and more sustainable manufacturing. The main incentive for applying

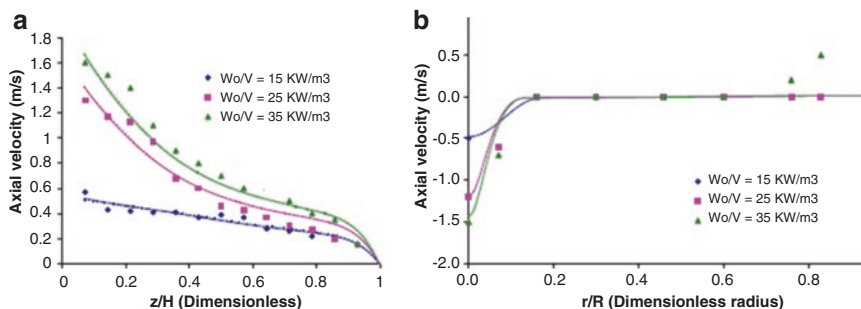


**Fig. 21.18** Quantitative comparison of model predictions and experimentally determined values of (a) the axial velocity at different height levels under the horn tip and (b) different radii at height level of 13% of the total reactor height

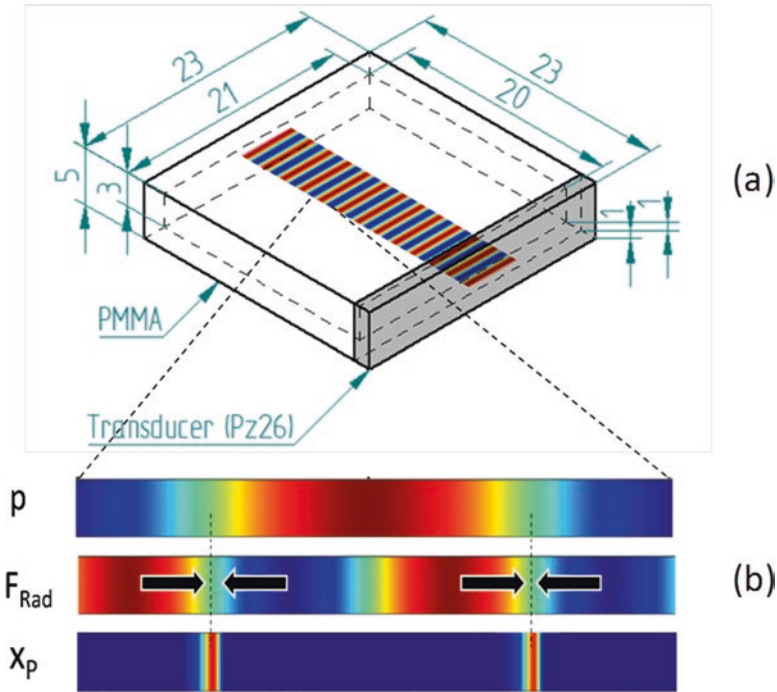


**Fig. 21.19** Schematic representation of the investigated treatment chamber with pressure distribution for a fixed frequency of 1.54 MHz (a), magnification of one wavelength of the pressure distribution (b;  $p$ ), the resulting acoustic force (b;  $F_{Rad}$ ) and the particles concentrated at the nodes of the pressure wave at the fixed frequency (b;  $X_p$ )

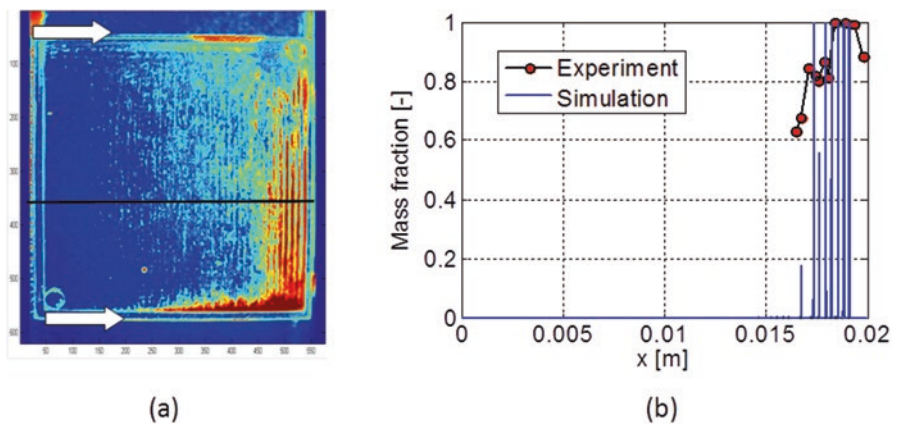


**Fig. 21.20** (a) Digitized image of actual process at a discrete time of 120 s (false color representation; the black line indicating the area for comparison with the model prediction); (b) comparison of the mass fraction of the separated particles measured and predicted

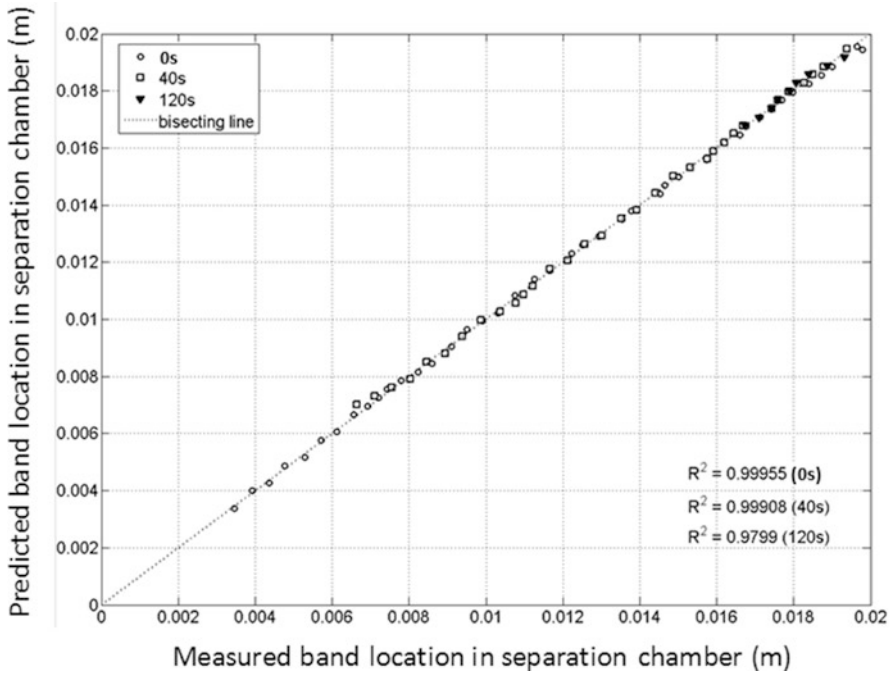


**Fig. 21.21** Parity plot of the measured and predicted band locations at discrete time steps of 0, 40, and 120 s

these new technologies should focus on inducing disruptive innovation in the food manufacturing industry rather than providing merely incremental improvements of existing processes.

Validated Multiphysics models have been used to characterize, evaluate, and optimize existing equipment for innovative food processing technologies and such modelling strategies will assist in further developing these technologies for effective and efficient implementation in the food manufacturing industry. Without such modelling capabilities, relying on the traditional approach of trial and error, development will be slow and in some instances a sufficient performance justifying utilization in industry may never happen.

## References

- Barbosa-Canovas GV, Albaali A, Juliano P, Knoerzer K (2011) Introduction to innovative food processing technologies: background, advantages, issues, and need for multiphysics modeling. In: Knoerzer K, Juliano P, Roupas P, Versteeg C (eds) *Innovative food processing technologies: advances in multiphysics simulation*. Wiley Blackwell, Ames, IA, pp 3–22
- Birla S, Wang S, Tang J (2008) Computer simulation of radio frequency heating of model fruit immersed in water. *J Food Eng* 84(2):270–280

- Buckow R, Schroeder S, Berres P, Baumann P, Knoerzer K (2010) Simulation and evaluation of pilot-scale pulsed electric field (PEF) processing. *J Food Eng* 101(1):67–77
- Buckow R, Baumann P, Schroeder S, Knoerzer K (2011) Effect of dimensions and geometry of co-field and co-linear pulsed electric field treatment chambers on electric field strength and energy utilisation. *J Food Eng* 105(3):545–556
- Buckow R, Semrau J, Sui Q, Wan J, Knoerzer K (2012) Numerical evaluation of lactoperoxidase inactivation during continuous pulsed electric field processing. *Biotechnol Prog* 28(5):1363–1375
- Day L, Xu M, Oiseth SK, Mawson R (2012) Improved mechanical properties of retorted carrots by ultrasonic pre-treatments. *Ultrason Sonochem* 19(3):427–434
- Geedipalli S, Rakesh V, Datta A (2007) Modeling the heating uniformity contributed by a rotating turntable in microwave ovens. *J Food Eng* 82(3):359–368
- Gogate PR, Kabadi AM (2009) A review of applications of cavitation in biochemical engineering/biotechnology. *Biochem Eng J* 44(1):60–72
- Heinz V, Toepfl S, Knorr D (2003) Impact of temperature on lethality and energy efficiency of apple juice pasteurization by pulsed electric fields treatment. *Innov Food Sci Emerg Technol* 4(2):167–175
- Huachen P, Orava M (2007) Performance evaluation of the UV disinfection reactors by CFD and fluence simulations using a concept of disinfection efficiency. *J Water Supply Res Technol* 56(3):181–189
- Juliano P, Knoerzer K, Fryer P, Versteeg C (2009) *C. botulinum* inactivation kinetics implemented in a computational model of a high pressure sterilization process. *Biotechnol Prog* 25(1):163–175
- Juliano P, Temmel S, Rout M, Swiergon P, Mawson R, Knoerzer K (2013) Creaming enhancement in a liter scale ultrasonic reactor at selected transducer configurations and frequencies. *Ultrason Sonochem* 20(1):52–62
- Knoerzer K, Chapman B (2011) Effect of material properties and processing conditions on the prediction accuracy of a CFD model for simulating high pressure thermal (HPT) processing. *J Food Eng* 104(3):404–413
- Knoerzer K, Juliano P, Gladman S, Versteeg C, Fryer P (2007) A computational model for temperature and sterility distributions in a pilot-scale high-pressure high-temperature process. *AIChE J* 53(11):2996–3010
- Knoerzer K, Regier M, Schubert H (2008) A computational model for calculating temperature distributions in microwave food applications. *Innov Food Sci Emerg Technol* 9(3):374–384
- Knoerzer K, Buckow R, Juliano P, Chapman B, Versteeg C (2010) Carrier optimisation in a pilot-scale high pressure sterilisation plant – an iterative CFD approach. *J Food Eng* 97(2):199–207
- Knoerzer K, Arnold M, Buckow R (2011a) Utilising multiphysics modelling to predict microbial inactivation induced by pulsed electric field processing. ICEF11 - 11th International Congress on Engineering and Food, Athens, Greece, 22–26 May 2011
- Knoerzer K, Juliano P, Roupas P, Versteeg C (2011b) Innovative food processing technologies: advances in multiphysics simulation. Wiley Blackwell, Ames, IA
- Knoerzer K, Baumann P, Buckow R (2012) An iterative modelling approach for improving the performance of a pulsed electric field (PEF) treatment chamber. *Comput Chem Eng* 37:48–63
- Kumar A, Kumaresan T, Pandit AB, Joshi JB (2006) Characterization of flow phenomena induced by ultrasonic horn. *Chem Eng Sci* 61(22):7410–7420
- Olivier S, Bull M, Stone G, Diepenbeek R, Kormelink F, Jacobs L, Chapman B (2011) Strong and consistently synergistic inactivation of spores of spoilage-associated *Bacillus* and *Geobacillus* spp. by high pressure and heat compared with inactivation by heat alone. *Appl Environ Microbiol* 77(7):2317–2324
- Rodríguez G, Riera E, Gallego-Juarez JA, Acosta VM, Pinto A, Martínez I, Blanco A (2010) Experimental study of defoaming by air-borne power ultrasonic technology. *Physics Procedia* 3(1):135–139
- Sabarez H, Gallego-Juarez J, Riera E (2012) Ultrasonic-assisted convective drying of apple slices. *Drying Technol* 30(9):989–997

- Tiwari G, Wang S, Tang J, Birla S (2011) Computer simulation model development and validation for radio frequency (RF) heating of dry food materials. *J Food Eng* 105(1):48–55
- Trujillo FJ, Knoerzer K (2009) An approach to model the acoustic streaming induced by an ultrasonic horn in a sonoreactor. Institute of Food Technologists (IFT) Annual Meeting and Food Expo, Anaheim, CA, USA, June 2009
- Trujillo FJ, Knoerzer K (2011) A computational modeling approach of the jet-like acoustic streaming and heat generation induced by low frequency high power ultrasonic horn reactors. *Ultrason Sonochem* 18(6):1263–1273
- Trujillo FJ, Eberhardt S, Moeller D, Dual J, Knoerzer K (2013) Multiphysics modelling of the separation of suspended particles via frequency ramping of ultrasonic standing waves. *Ultrason Sonochem* 20(2):655–666
- Unluturk SK, Arastoopour H, Koutchma T (2004) Modeling of UV dose distribution in a thin-film UV reactor for processing of apple cider. *J Food Eng* 65(1):125–136